



# Structure characterization of an exopolysaccharide produced by *Bifidobacterium animalis* RH

Nan Shang<sup>b</sup>, Rihua Xu<sup>a,b,\*</sup>, Pinglan Li<sup>b</sup>

<sup>a</sup> College of Life Science, Inner Mongolia University, Hohhot 010021, PR China

<sup>b</sup> Key Lab of Functional Dairy, College of Food Science and Nutritional Engineering, China Agricultural University, Beijing 100083, PR China

## ARTICLE INFO

### Article history:

Received 1 June 2012

Received in revised form 23 July 2012

Accepted 3 August 2012

Available online 14 August 2012

### Keywords:

*Bifidobacterium animalis*

Exopolysaccharides

Purification

Structure

## ABSTRACT

An exopolysaccharide fraction (EPSb) produced by *Bifidobacterium animalis* RH isolated from the feces of centenarians was purified to illustrate its structure and conformational characterization. Results from Fourier-transform infrared spectrometry, gel permeation chromatography, high-pH anion-exchange chromatography with pulsed amperometric detection, periodate oxidation and Smith degradation, methylation and gas chromatography–mass spectrometry, and nuclear magnetic resonance analysis indicated that EPSb ( $M_w = 21.3$  kDa) was composed of rhamnose (Rha), arabinose (Ara), galactose (Gal), glucose (Glc), and mannose (Man) in a molar ratio of 0.4:0.3:1.6:0.8:1.2. This compound had a backbone of (1 → 3,4)-linked Man, (1 → 4)-linked Rha, (1 → 4)-linked Gal, and (1 → 4)-linked Glc. It was branched with Gal and terminated with Gal and Glc residues. The molecular structure of EPSb was observed via atomic force microscopy. EPSb showed spherical lumps and a ring-like network. Conformational analysis revealed the non-triple helical conformation of EPSb.

© 2012 Elsevier Ltd. All rights reserved.

## 1. Introduction

The human large intestine contains a complex microflora. Bifidobacteria are often the predominant species in the gut microbiota of healthy humans. Aside from their wide range of therapeutic values in humans, these microorganisms have long been recognized as bacteria with probiotic, nutritive, and therapeutic properties. The health and nutritional benefits ascribed to bifidobacteria include maintenance of healthy intestinal microflora and integrity, improvement of lactose digestibility and tolerance, antitumorigenic activity, reduction of serum cholesterol levels, synthesis of B-complex vitamins, and absorption of calcium (Hoover, 1993).

Several lactic acid bacteria (LAB) produce exopolysaccharides (EPSs) that are secreted into the growth media. Since 1990, several structural studies and functionality of EPSs produced by different strains of LAB have been reported (Frengova, Simova, & Beshkova, 1997). The production of EPS is a relatively novel characteristic in the genus *Bifidobacterium*. Given that bifidobacteria are obligated anaerobes, certain precautions are required to prevent the toxic effects of oxygen when they are cultivated for industrial applications. Thus, compared with the genera *Lactobacillus*, *Streptococcus*,

and *Lactococcus*, little is known on the structure and bioactivities of EPS produced by the genus *Bifidobacterium*. Structures of the cell wall polysaccharides from *Bifidobacterium longum* YIT4016 and *Bifidobacterium catenulatum* YIT4028 (Nagaoka et al., 1995, 1996), as well as EPSs from *Bifidobacterium longum* have been reported (Robert, 1995; Andaloussi, 1995). They were all heteropolysaccharides composed of galactose (Gal), glucose (Glc), and rhamnose (Rha), among others.

Several lactobacilli and bifidobacteria used as probiotic bacteria produce EPSs. The health-promoting effect of EPS-producing strains is suggested to be related to the biological activities of these biopolymers. EPSs are beneficial to human health as probiotics because of their anti-tumor, anti-ulcer, immunomodulating, and cholesterol-lowering activities (Ruas-Madiedo, Hugenholtz, & Zoon, 2002). The molecular structure and conformation of polysaccharides are important in determining the bioactivities of these compounds (Ye, Wang, Zhou, Liu, & Zeng, 2008; Tao, Zhang, & Cheung, 2006; Qi, Zhang, Zhao, Chen, & Zhang, 2005).

New technologies, such as atomic force microscopy (AFM) and laser light scattering, have emerged as powerful tools for single-molecule force spectroscopy experiments and microcosmos observation. These techniques can be used to characterize the surface structures and molecular weight of aqueous samples (Chen et al., 2009). AFM has recently been used to study the molecular structure of some polysaccharides (Zhang et al., 2007; Iijima, Shinozaki, Hatakeyama, Takahashi, & Hatakeyama, 2007; Ikeda & Shishido, 2005). However, studies on EPSs produced by LAB, especially bifidobacterium, are lacking.

\* Corresponding author at: College of Life Sciences, Inner Mongolia University, 235 Daxue West Road, Hohhot 010021, Inner Mongolia, PR China.

Tel.: +86 471 4991676; fax: +86 471 4991436.

E-mail address: [xurihua81@126.com](mailto:xurihua81@126.com) (R. Xu).

We isolated an EPS-producing strain *B. animalis* RH from the feces of centenarians in Bama (Guangxi, China), which was listed as one of the five officially certified villages of longevity by the International Society of Natural Medicine in 1991. To the best of our knowledge, only a few studies have focused on the structure, especially conformational analysis, of EPS from *B. animalis*. Accordingly, in the present study, we reported the chemical structure and conformational characterization of EPSb, one of the fractions from *B. animalis* RH.

## 2. Materials and methods

### 2.1. Materials and reagents

*B. animalis* RH was isolated from the feces of Bama centenarians. The strain was isolated by plating on solid, calcium carbonate-containing (0.3%, w/v) MRS medium after 10-fold serial dilution (Xu, Ma, Wang, Liu, & Li, 2010).

Monosaccharide and dextran were purchased from Sigma–Aldrich (Shanghai, China). DEAE-Sephacrose fast flow and Sepharose CL-6B were obtained from the Pharmacia Company (Beijing, China). D-Glucuronic acid was purchased from Chem-synlab Co., Ltd. (Beijing, China). Analytical-grade BaCO<sub>3</sub>, NaIO<sub>4</sub>, NaBH<sub>4</sub>, and FeSO<sub>4</sub> were purchased from Beijing Chemicals Co., Ltd.

### 2.2. Production, isolation, and purification of the EPS

*B. animalis* RH was cultured at 37 °C under anaerobic conditions in peptone, tryptone, yeast extract, and glucose (PTYG) medium (containing 5 g of peptone, 5 g of tryptone, 10 g of yeast extract, 10 g of glucose, 0.1 mL of Tween 80, 0.05 g L-cysteine monohydrochloride, and 4 mL of saline solution per liter of water; pH 6.8–7.0; saline solution contained 0.2 g of CaCl<sub>2</sub>, 1.0 g of KH<sub>2</sub>PO<sub>4</sub>, 0.48 g of MgSO<sub>4</sub>·7H<sub>2</sub>O, 10 g of NaCO<sub>3</sub>, and 2.0 g of NaCl per liter of water) for 48 h without pH control. After incubation, the EPS was isolated and purified as previously described (Xu, Shen, Ding, Gao, & Li, 2011). Briefly, cells were removed from the culture medium via centrifugation at 8000 × g for 10 min at 4 °C. After discarding the pellet, the supernatant was concentrated and then precipitated with three volumes of 95% (vol/vol) cold ethanol overnight at 4 °C. The crude EPS was collected via centrifugation at 8000 × g for 10 min and dissolved in distilled water (50%, w/v). The solution was treated with Sevag agent (chloroform:n-butanol = 4:1) and centrifuged to remove free protein. The supernatant was dialyzed using a dialysis bag (*M<sub>w</sub>* cut-off 8 kDa to 14 kDa) against distilled water for 48 h at 4 °C with water replacement twice a day. Finally, the EPS was fractionated through anion exchange chromatography on DEAE-Sephacrose Fast Flow (2.6 cm × 20 cm) with a linear gradient of NaCl concentration (0–1 M) and then further purified via gel permeation chromatography (GPC) using a Sepharose CL-6B column (160 cm × 80 cm) eluted with 50 mM NaCl (30 mL/h). The fractions were tested for carbohydrate content through the phenol–sulfuric acid method using Glc as standard (Dubois, Gilles, Hamilton, Rebers, & Smith, 1956) and for peptide content via UV absorption at 280 nm. The fractions were collected separately according to the carbohydrate elution profile and lyophilized after dialysis against distilled water.

### 2.3. Molecular mass determination

The molecular weight of the EPS was determined through GPC, in combination with a high-performance liquid chromatography instrument (Knauer, Germany). The sample (1.0 mg/mL) was passed through a 0.45 μm filter, applied to a gel-filtration chromatographic column of Shodex Sugar KS-805 (SHOWA DENKI Co., Ltd, Japan), kept at 60 °C, eluted with 0.1 M sodium nitrate at a flow

rate of 0.5 mL/min, and detected using a refractive index detector. The molecular weight was calculated by the calibration curve obtained using various standard dextrans (*M<sub>w</sub>*: 1400, 670, 270, 50, 12, and 5 kDa, Sigma) (Luo, 2008).

### 2.4. Spectral analysis

Fourier-transform infrared spectra (FT-IR) of EPSb were obtained using a NEXUS-470 FT-IR spectrometer (Nicolet Nexus, USA) to detect functional groups. The purified polysaccharides (1 mg) was ground with KBr (spectroscopic grade) powder and then pressed into pellets for FT-IR measurement in the frequency range of 4000–400 cm<sup>−1</sup>.

Nuclear magnetic resonance (NMR) spectra were obtained on a JEOL JNM-ECA600 spectrometer at 27 °C. The samples were deuterium-exchanged several times by freeze-drying from <sup>2</sup>H<sub>2</sub>O and then examined in solution (~100 mg/1 mL).

### 2.5. Monosaccharide analysis

The EPS was hydrolyzed with 12 M H<sub>2</sub>SO<sub>4</sub> at 100 °C for 2.5 h. The hydrolyzates were obtained by filtration and centrifugation at 4000 × g for 10 min after they were neutralized to pH 6.0 with BaCO<sub>3</sub>. The supernatant was diluted 20 times and fractionated by high-pH anion-exchange chromatography with pulsed amperometric detection (HPAEC-PAD) on a Dionex system (Ai et al., 2008). The DIONEX-2500 ion chromatograph was equipped with a CarboPac PA20 sugar column. The column was eluted with a mixture of water and 200 mM NaOH in the volume ratio of 91:9 at a flow rate of 1.0 mL/min. Standard Glc, Gal, Rha, mannose (Man), fructose, and arabinose (Ara) (Sigma, ≥99%) were prepared for comparison.

### 2.6. Periodate oxidation and Smith degradation

EPS (20 mg) was dissolved in 12.5 mL of distilled water and mixed with 12.5 mL of 30 mM NaIO<sub>4</sub> to a final concentration of 15 mM. The mixture was kept in the dark at 4 °C. Subsequently, 200 μL aliquots were withdrawn every 8 h, diluted 250 times with distilled water, and read in a spectrophotometer at 223 nm. Ethylene glycol (2 mL) was added to terminate the reaction after 10 d. Approximately 2 mL of the periodate-oxidized product was used to calculate the yield of formic acid by 0.00946 M NaOH. The rest was dialyzed against distilled water for 48 h. Afterwards, the content inside the dialysis sack was concentrated and reduced overnight with NaBH<sub>4</sub>, neutralized with 50% acetic acid, and dialyzed against distilled water for 24 h. Then one-third of the solution was concentrated, freeze-dried, and fully hydrolyzed for gas chromatographic (GC) analysis. The rest was added to the same volume of 1 M H<sub>2</sub>SO<sub>4</sub>, kept for 40 h at 25 °C, neutralized to pH 6.0 with BaCO<sub>3</sub>, and filtered for Smith degradation analysis. The filtrate was dialyzed for 48 h. The content out of sack was desiccated for GC analysis, and the content inside was precipitated with ethanol. The supernatant and precipitate were also dried out for GC analysis after centrifugation (Wang, Luo, & Liang, 2004). Finally, the obtained fractions were hydrolyzed with 2 M TFA at 120 °C for 1 h, converted into alditol acetates as described by Jacob (Jacob, 1985), and analyzed via GC. GC was performed on an Agilent 4890 instrument (Agilent, USA) equipped with an HP-5 column (0.53 mm × 15 m) and a flame ionization detector using a temperature program of 60–260 °C at a rate of 15 °C/min.

### 2.7. Methylation analysis

The EPS sample (7 mg) was permethylated using methyl iodide and solid NaOH in dimethyl sulfoxide (Ciucanu & Kerek, 1984). The permethylated EPS was hydrolyzed with 2 M TFA at 120 °C for 1 h.

The partially methylated monosaccharides obtained were reduced with  $\text{NaBH}_4$ , followed by neutralization by acetic acid and removal of boric acid by reduced pressure evaporation. Finally, the EPS sample was acetylated with 1:1 pyridine–acetic anhydride (1 h,  $100^\circ\text{C}$ ) to yield mixtures of partially methylated alditol acetates, which were analyzed via GC–mass spectrometry (GC–MS). GC–MS analysis was performed on a Varian 450–GC/320–MS system using a VF-5 column ( $0.25\ \mu\text{m} \times 0.25\ \text{mm} \times 30\ \text{m}$ ) at a temperature program of  $50\text{--}290^\circ\text{C}$  and a rate of  $10^\circ\text{C}/\text{min}$ . Helium was used as carrier gas.

## 2.8. Helix-coil transition analysis

The Congo red–EPS complexes were characterized according to the method described by Ogawa and Hatano (1978) to establish the conformational structure. Solutions of the EPSb sample (5 mg/2 mL) in 0.0–0.4 M NaOH (increasing stepwise by 0.05 M increments) were prepared containing  $91\ \mu\text{M}$  of Congo red. After a 3 h reaction, the visible absorption spectra were obtained from 480 nm to 510 nm at  $25^\circ\text{C}$  using a Tu-1901 double beam UV/visible spectrophotometer. Congo red in NaOH served as the negative control.

## 2.9. Imaging with AFM

EPSb was imaged with AFM according to Chen et al. (2009). A stock solution (1.0 mg/mL) was prepared by adding purified EPSb into  $\text{ddH}_2\text{O}$ . The solution was diluted to a final concentration of 0.01 mg/mL. Samples ( $5\ \mu\text{L}$ ) were deposited onto freshly cleaved mica sheets, allowed to dry, and then imaged in air at room temperature. Images were obtained using a Dimension-3100 instrument (Digital Instruments Co., USA) in the tapping mode. The resulting imaging force was estimated to be 3–4 nN, and the resonant frequency was approximately 2 kHz.

## 3. Results and discussion

### 3.1. Isolation, purification, and composition of EPS

EPSs obtained from media culture of *B. animalis* RH were fractionated into two peaks through anion exchange chromatography (data not shown) and named as EPSa and EPSb. The EPSb fractions corresponding to the second peak were involved in this study because they possessed high anti-tumor activity in vitro (data not shown). The analysis of gel permeation chromatography revealed the presence of one peak, indicating the homogeneity of the EPSb fraction. This fraction was collected, dialyzed with distilled water, and lyophilized for further study.

The molecular mass was calculated as 21.3 kDa according to the standard curve equation  $\text{Log } M_p = 14.1795 - 0.5185t$  ( $R^2 = 0.9763$ ), where  $M_p$  is the peak molecular weight and  $t$  is the retention time. The value was smaller than the EPS (greater than 200 kDa) isolated from *B. longum* BB-79 (Robert, 1995) and two subfractions (0.36 and 1.2 MDa) of *B. longum* (Andaloussi, 1995).

Determination of monomer composition was carried out after acid hydrolysis. Quantitative monosaccharide analysis of the EPS revealed the presence of Rha, Ara, Gal, Glc, and Man in molar ratios of 0.4:0.3:1.6:0.8:1.2 compared with the HPAEC spectra of standard monosaccharides (Fig. 1A and B). The sugar composition suggested that the EPS was a heteropolysaccharide, which was composed of a backbone of repeated subunits and consist of three to eight monosaccharides. The constituting monosaccharides seem to be similar to other EPSs produced by lactic acid bacteria (Ruas-Madiedo et al., 2002). However, the low content of L-arabinose may be due to the noise created by instruments.

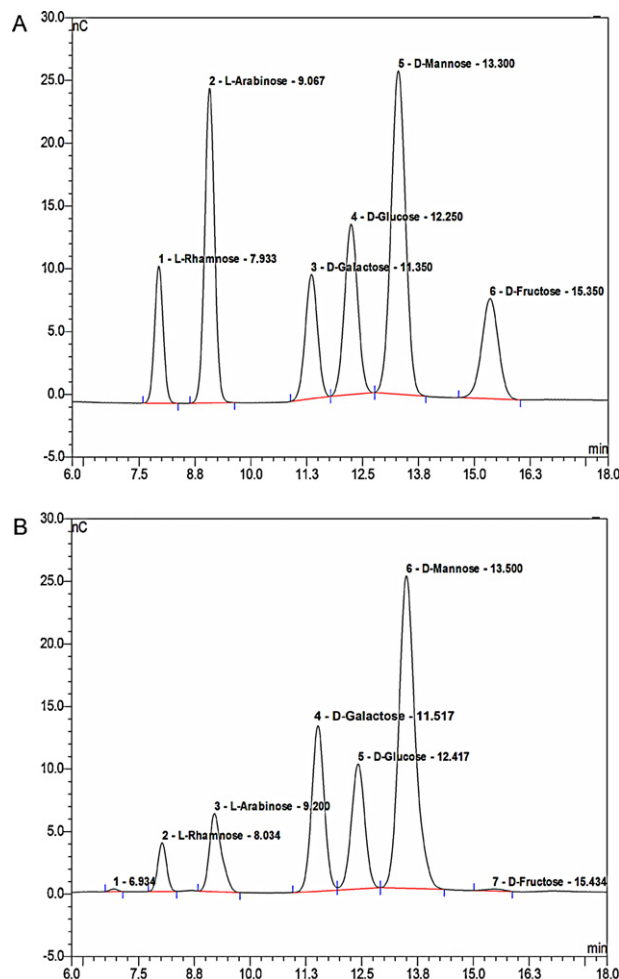


Fig. 1. Chromatogram of standard monosaccharide (A) and EPSb monosaccharide compositions (B) on HPAEC–PAD.

### 3.2. Structural analysis

The FT–IR spectra of purified EPS fractions are illustrated in Fig. 2. The result showed characteristic absorbance of polysaccharides. The intensity of bands in the region  $3600\text{--}3200\ \text{cm}^{-1}$  was due to the hydroxyl stretching vibration of the polysaccharide, which was expected to be broad. The absorption bands at  $2988.4\ \text{cm}^{-1}$  in the range of  $3200\text{--}2800\ \text{cm}^{-1}$  were due to the C–H stretching vibration. Each polysaccharide showed high absorbance in the region  $1200\text{--}950\ \text{cm}^{-1}$ , which was within the so-called fingerprint region. Hence, in the fingerprint region, the strongest absorption band at  $1038.3\ \text{cm}^{-1}$  indicates that the substance is polysaccharide and suggests that the monosaccharide in it has a pyranose ring (Sheng et al., 2007; Wei, Zhou, Zang, & Jiang, 2007). The peaks at 1554.1, 1463.1, and  $1403.2\ \text{cm}^{-1}$  were characteristic of the carboxyl groups or carboxylate, indicating that EPSb is an acidic polysaccharide. This result is consistent with its uronic acid content (approximately 14%) quantified through the carbazole–sulfuric acid method using D-glucuronic acid as standard (Dische, 1947). Moreover, the characteristic absorptions at  $843.1\ \text{cm}^{-1}$  indicate that  $\alpha$ -configurations exist in the polysaccharides (Ye et al., 2009).

The results of periodate oxidation showed that 1.012 mmol periodate was consumed, and 0.058 mmol formic acid was produced per sugar residue. This finding indicates the existence of a small amount of  $1\rightarrow$  linked or  $1\rightarrow 6$  linked monosaccharides. The full acid hydrolysis of the periodate-oxidized products and three fractions after partial acid hydrolysis (precipitate and supernatant

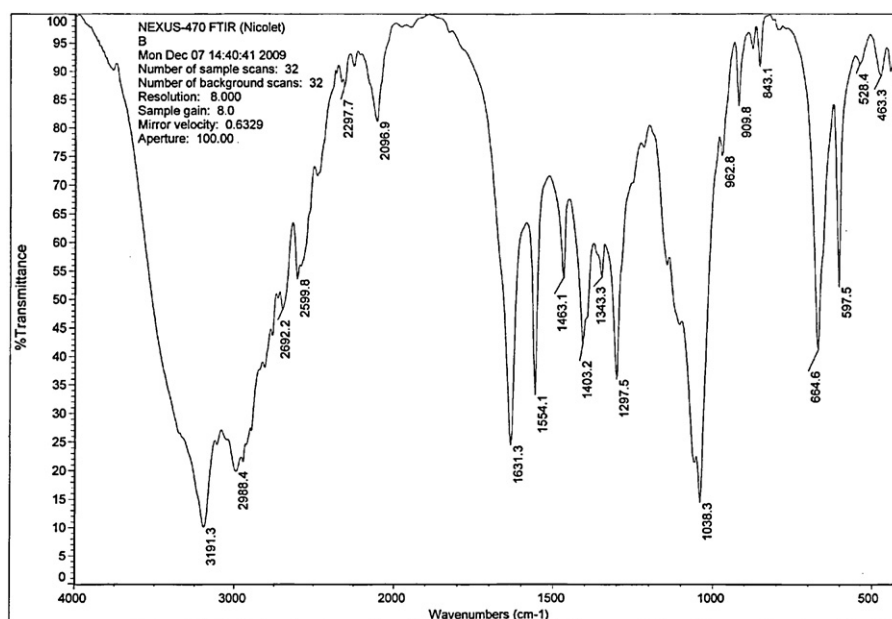


Fig. 2. FT-IR spectra of EPSb isolated from *Bifidobacterium animalis* RH.

Table 1

The results of periodate oxidation and Smith degradation of EPSb.

Periodate oxidation						
Consumption of HIO <sub>4</sub> (mmol)						0.124
Consumption of HIO <sub>4</sub> /hexose (mol/mol)						1.012
Amount of formic acid (mmol)						0.0071
Amount of formic acid/hexose (mol/mol)						0.058
Smith degradation						
Fractions	Glucose	Galactose	Mannose	Rhamnose	Glycerol	Erythritol
Full acid hydrolysis	— <sup>a</sup>	—	+ <sup>b</sup>	—	+	+
Out of sack	+	+	—	+	+	+
Supernatant in the sack	—	—	—	—	—	—
Precipitation in the sack	—	—	—	—	—	—

<sup>a</sup> Undetectable on gas chromatogram.

<sup>b</sup> Detectable on gas chromatogram.

in the dialysis sack, whereas fraction out of the dialysis sack was obtained and subjected to GC analysis (Table 1). The existence of Man in full acid hydrolysis revealed that (1→3)-linked, (1→2,3)-linked, (1→2,4)-linked, (1→3,4)-linked, (1→2,3,4)-linked, (1→3,6) linked, or (1→2,3,6)-linked Man residues could not be oxidized by sodium periodate (HIO<sub>4</sub>). No Glc, Gal, and Rha were observed, and a large amount of glycerol and erythritol was obtained. This result demonstrates that they were in linkages that can be oxidized, namely, 1→, (1→6), (1→2), (1→2,6), (1→4), or (1→4,6) linkage. The results of Smith degradation analysis are summarized in Table 1. The existence of Glc, Gal, and Rha out of the dialysis sack also indicates that these residues can be oxidized by HIO<sub>4</sub> and that some of these compounds could be the branched structure of EPSb. No precipitates in the sack and no substances in the supernatant of the sack were observed. This finding suggests that the linkages of the backbone of EPSb should have been all oxidized by HIO<sub>4</sub>. In addition, the linkages that cannot be oxidized should have not been arranged continuously.

The fully methylated EPSb was hydrolyzed with acid, converted into alditol acetates, and analyzed via GC–MS (Table 2). The results showed the presence of six components, namely 2,3,4-Me<sub>3</sub>-Gal, 2,5-Me<sub>2</sub>-Man, 2,3,5-Me<sub>3</sub>-Rha, 2,3,4,6-Me<sub>3</sub>-Glc, 2,3,6-Me<sub>3</sub>-Glc, and 2,3,6-Me<sub>3</sub>-Gal in molar ratios of 2.5:2.8:1.3:1.4:1.9:1.5. This phenomenon showed a correlation between terminal and branched residues, and the molar ratios corresponded to the

monosaccharide composition described above. The molar ratio of (1→3,4)-linked Man and 1→ linked Gal was twice as much as the other monomers. Hence, 2,5-Me<sub>2</sub>-Man (1→3, 4-linked Man) linked with 2,3,4-Me<sub>3</sub>-Gal (1→ linked Gal) was the major component of the repeating units. The results from GC–MS, partial acid hydrolysis, periodate oxidation, and Smith degradation indicated that 2,5-Me<sub>2</sub>-Man was the only linkage that could be oxidized by HIO<sub>4</sub>. In addition, 2,5-Me<sub>2</sub>-Man was in the backbone structure and arranged twice. The linkages that could be oxidized were sequenced discontinuously, and the residues of the branches were terminated with Gal and Glc.

Table 2

Methylation analysis of the EPSb by GC–MS.

Retention time (min)	Methylated sugars <sup>a</sup>	Linkage types	Molar ratio
11.916	2,3,4-Me <sub>3</sub> -Gal	α-D-Galp-(1→	2.5
13.545	2,5-Me <sub>2</sub> -Man	→3,4)-D-Manf-(1→	2.8
15.613	2,3,5-Me <sub>3</sub> -Rha	→4)-L-Rha-(1→	1.3
21.202	2,3,4-Me <sub>3</sub> -Glc	→6)-α-D-Glcp-(1→	1.4
22.858	2,3,6-Me <sub>3</sub> -Glc	→4)-D-Galf-(1→	2.1
24.025	2,3,6-Me <sub>3</sub> -Gal	→4)-α-D-Glcp-(1→	1.8

<sup>a</sup> 2,3,6-Me<sub>3</sub>-Gal = 1,4-di-O-acetyl-2,3,6-tri-O-methyl-galactose, etc.



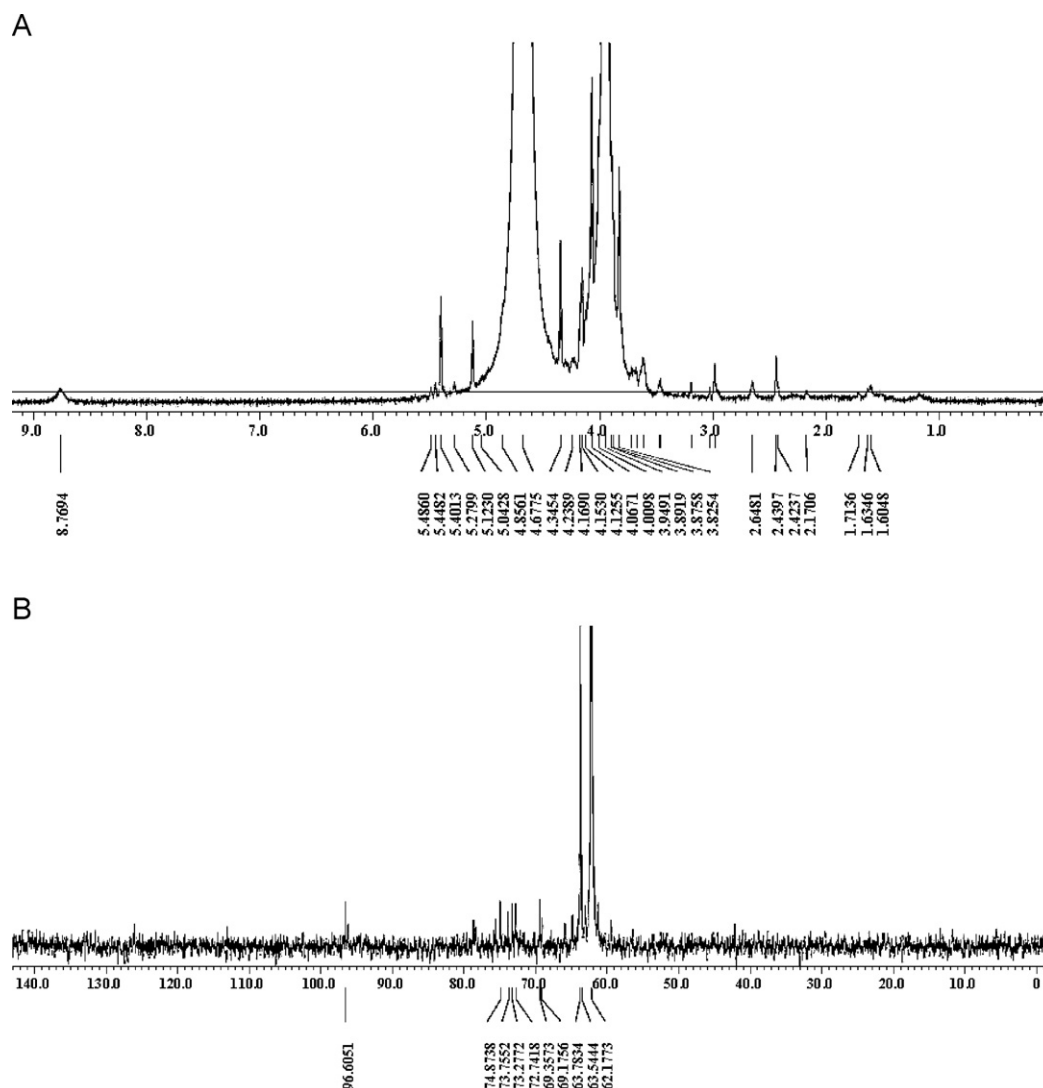


Fig. 3. 600 MHz  $^1\text{H}$  NMR (A) and  $^{13}\text{C}$  NMR (B) spectra of the EPSb from *B. animalis* RH.

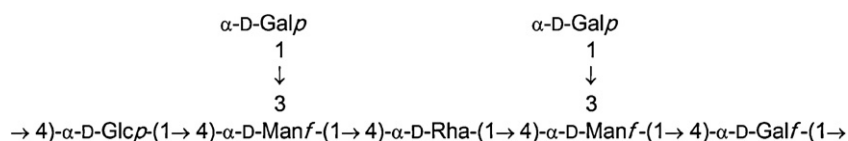


Fig. 4. Predicted structure of the EPSb monomer.

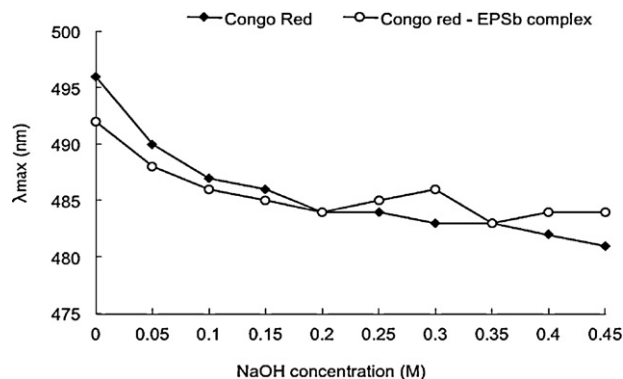


Fig. 5. Variation in the maximum absorption of the Congo red-EPSb complex at various concentrations of sodium hydroxide solution.

Signals in the  $^1\text{H}$  NMR and  $^{13}\text{C}$  NMR spectra of the EPSb were assigned as completely as possible based on component and methylation analyses, as well as literature values. The  $^1\text{H}$  NMR spectrum (Fig. 3A) of EPSb showed seven signals in the anomeric region ( $\delta$  4.5–5.5), suggesting a heptasaccharide repeating unit. The signal in the anomeric region corresponds to C-1 of  $\alpha$ -type configuration. No high-field anomeric resonance, characteristic of  $\beta$ -linked glycosyl residues was observed. The  $^{13}\text{C}$  NMR spectrum (Fig. 3B) showed the anomeric proton at  $\delta$  96.61, which can be attributed to the  $\alpha$ -anomer, whereas the other protons appeared as a complex series of overlapping signals in the  $\delta$  60–75 range.

The results suggest that EPSb has a backbone of (1  $\rightarrow$  3,4)-linked Man, (1  $\rightarrow$  4)-linked Rha, (1  $\rightarrow$  4)-linked Gal, and (1  $\rightarrow$  4)-linked Glc, branched with Gal and terminated with Gal and Glc residues. In summary, the monomer of EPSb is evaluated in Fig. 4.

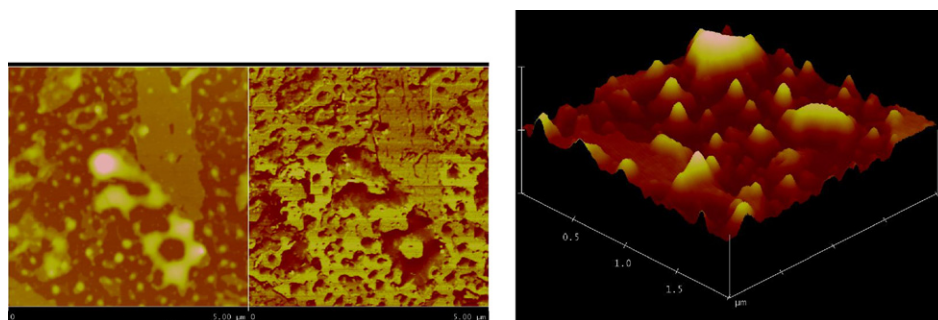


Fig. 6. AFM images of EPSb.

### 3.3. Conformational characterization

Polymers that exist in an ordered conformation (triplex) can form a complex with Congo red in diluted aqueous NaOH solutions, determining a shift in the maximum adsorption wavelength ( $\lambda_{\max}$ ). The formation of these complexes and the resulting shift of  $\lambda_{\max}$  value is a rapid method for detecting helical structures. The greater the effect in the  $\lambda_{\max}$  shift, the higher the helical structure content is. Thus, helices can be destroyed by adding sodium hydroxide, which rapidly causes a loss of interaction between the polysaccharide and Congo red (Kulicke, Lettau, & Thielking, 1997). In this way, a shift in the maximum visible absorption of Congo red induced by the presence of a polysaccharide was used for conformational studies. In this study, the transition of the triple-helical arrangement to the single-stranded conformation was studied by measuring the  $\lambda_{\max}$  for Congo red-EPSb solutions at NaOH concentrations ranging from 0.05 M to 0.4 M. The same behavior was observed for both Congo red-EPSb solution and Congo red negative control. This result demonstrates the absence of a triple-helical conformation in EPSb (Fig. 5).

Images of EPSb deposited on mica were obtained via AFM (Fig. 6A and B). Many irregularly ranged spherical lumps were apparent, and large worm-like or ring-like structures were formed. The diameter of spherical lumps ranged from 300 nm to 500 nm, and the height varied from 1 nm to 5 nm. These sizes were much larger than that of a single polysaccharide chain (approximately 0.1–1 nm), suggesting that inter- and/or intra-molecular aggregation might be involved, and a tangled network is formed. In detail, some regions had large aggregates like a fibrous network, whereas other regions were characterized by complex branched fibers. This finding suggests that these worm-like or ring-like structures might be tangled networks. In addition, EPSb is a negatively charged polysaccharide because of the carboxyl groups, and mica is a type of aluminum silicate that is also negative. Thus, a repulsive force may be present between EPSb and mica, causing the formation of a ball-like image.

## 4. Conclusion

A few studies have reported on the structural and conformational studies of EPS produced by strictly anaerobic bacteria. To the best of our knowledge, the present study is the first to report the structure characterization of EPS produced by *B. animalis*. In this study, EPSb was a highly branched heteropolysaccharide consisting of (1 → 4)-linked Glc, (1 → 3,4)-linked Man, (1 → 4)-linked Rha, and (1 → 4)-linked Gal, terminated with Glc and Gal, and Gal was distributed in branches. The AFM images illustrated that EPSb molecules have spherical lump and ring-like or worm-like morphologies. The Congo red test showed the absence of a triple-helical structure in EPSb.

## Acknowledgements

This research was funded by the Beijing Natural Science Foundation (5122018) and the Program of Higher-level talents of Inner Mongolia University (SPH-IMU, 115114).

## References

- Ai, L., Zhang, H., Guo, B., Chen, W., Wu, Z., & Wu, Y. (2008). Preparation, partial characterization and bioactivity of exopolysaccharides from *Lactobacillus casei* LC2W. *Carbohydrate Polymer*, 74, 353–357.
- Andaloussi, S. A. (1995). Isolation and characterization of exocellular polysaccharides produced by *Bifidobacterium longum*. *Applied Microbiology and Biotechnology*, 43, 995–1000.
- Chen, H. X., Wang, Z. S., Qu, Z. S., Fu, L. L., Dong, P., & Zhang, X. (2009). Physicochemical characterization and antioxidant activity of a polysaccharide isolated from oolong tea. *European Food Research and Technology*, 229, 629–635.
- Ciucanu, I., & Kerek, F. (1984). A simple and rapid method for the permethylation of carbohydrate. *Carbohydrate Research*, 131, 209–217.
- Dische, Z. (1947). A new specific color reaction of hexuronic acids. *Journal of Biological Chemistry*, 167, 189–198.
- Dubois, M., Gilles, K. A., Hamilton, J. K., Rebers, P. A., & Smith, F. (1956). Colorimetric method for determination of sugars and related substances. *Analytical Chemistry*, 28, 350–356.
- Frengova, G., Simova, E., & Beshkova, D. (1997). Caroteno-protein and exopolysaccharide production by cocultures of *Rhodotorula glutinis* and *Lactobacillus helveticus*. *Journal of Industrial Microbiology and Biotechnology*, 18, 272–277.
- Hoover, D. G. (1993). Bifidobacteria: Activity and potential benefits. *Food Technology*, 47, 120–124.
- Iijima, M., Shinozaki, M., Hatakeyama, T., Takahashi, M., & Hatakeyama, H. (2007). AFM studies on gelation mechanism of xanthan gum hydrogels. *Carbohydrate Polymer*, 68, 701–707.
- Ikeda, S., & Shishido, Y. (2005). Atomic force microscopy studies on heat-induced gelation of curd. *Journal of Agricultural and Food Chemistry*, 53, 786–791.
- Jacob, L. (1985). Simultaneous gas–liquid chromatographic determination of aldonic acids and aldoses. *Analytical Chemistry*, 57, 346–348.
- Kulicke, W.-M., Lettau, A. I., & Thielking, H. (1997). Correlation between immunological activity, molar mass, and molecular structure of different (1 → 3)- $\beta$ -D-glucans. *Carbohydrate Research*, 297, 135–143.
- Luo, D. (2008). Identification of structure and antioxidant activity of a fraction of polysaccharide purified from *Dioscorea nipponica* Makino. *Carbohydrate Polymer*, 71, 544–549.
- Nagaoka, M., Shibata, H., Kimura, I., Hashimoto, S., Kimura, K., Sawada, H., & Yokokura, T. (1995). Structural studies on a cell wall polysaccharide from *Bifidobacterium longum* YIT4028. *Carbohydrate Research*, 274, 245–249.
- Nagaoka, M., Hashimoto, S., Shibata, H., Kimura, I., Kimura, K., Sawada, H., & Yokokura, T. (1996). Structure of a galactan from cell walls of *Bifidobacterium catenulatum* YIT4016. *Carbohydrate Research*, 281, 285–291.
- Ogawa, K., & Hatano, M. (1978). Circular dichroism of the complex of a (1 → 3)- $\beta$ -D-glucan with Congo Red. *Carbohydrate Research*, 67, 527–535.
- Qi, H. M., Zhang, Q. B., Zhao, T. T., Chen, R., & Zhang, H. (2005). Antioxidant activity of different sulfate content derivatives of polysaccharide extracted from *Ulva pertusa* (Chlorophyta) in vitro. *International Journal of Biological Macromolecules*, 37, 195–199.
- Robert, C. M. (1995). Exopolysaccharide production by *Bifidobacterium longum* 88-79. *Journal of Applied Bacteriology*, 78, 463–468.
- Ruas-Madiedo, P., Hugenholtz, J., & Zoon, P. (2002). An overview of the functionality of exopolysaccharides produced by lactic acid bacteria. *International Dairy Journal*, 12, 163–171.
- Sheng, J., Yu, F., Xin, Z., Zhao, L., Zhu, X., & Hu, Q. (2007). Preparation, identification and their antitumor activities in vitro of polysaccharides from *Chlorella pyrenoidosa*. *Food Chemistry*, 105, 533–539.

- Tao, Y. Z., Zhang, L. N., & Cheung, P. C. K. (2006). Physicochemical properties and anti-tumor activities of water-soluble native and sulfated hyperbranched mushroom polysaccharides. *Carbohydrate Research*, 341, 2261–2269.
- Wang, Z. J., Luo, D. H., & Liang, Z. Y. (2004). Structure of polysaccharides from the fruiting body of *Hericium erinaceus* Pers. *Carbohydrate Polymer*, 57, 241–247.
- Wei, W. X., Zhou, W., Zang, N., & Jiang, L. B. (2007). Structural analysis of a polysaccharide from *Fructus Mori Albae*. *Carbohydrate Polymer*, 70, 341–344.
- Xu, R. H., Ma, S. M., Wang, Y., Liu, L. S., & Li, P. L. (2010). Screening, identification and statistic optimization of a novel exopolysaccharide producing *Lactobacillus paracasei* HCT. *African Journal of Microbiology Research*, 4, 783–795.
- Xu, R. H., Shen, Q., Ding, X. L., Gao, W. G., & Li, P. L. (2011). Chemical characterization and antioxidant activity of an exopolysaccharide fraction isolated from *Bifidobacterium animalis* RH. *European Food Research and Technology*, 232, 231–241.
- Ye, H., Wang, K. Q., Zhou, C. H., Liu, J., & Zeng, X. X. (2008). Purification, antitumor and antioxidant activities in vitro of polysaccharide from the brown seaweed *Sargassum Pallidum*. *Food Chemistry*, 111, 428–432.
- Ye, L. B., Zhang, J. S., Yang, Y., Zhou, S., Liu, Y. F., & Tang, Q. J. (2009). Structural characterisation of a heteropolysaccharide by NMR spectra. *Food Chemistry*, 112, 962–966.
- Zhang, J., Wu, J., Liang, J. Y., Hu, Z. A., Wang, Y. P., & Zhang, S. T. (2007). Chemical characterization of Artemisia seed polysaccharide. *Carbohydrate Polymer*, 67, 213–218.